Progress In Electromagnetics Research, Vol. 140, 241–261, 2013

ELECTRONICALLY RECONFIGURABLE BEAM STEERING ANTENNA USING EMBEDDED RF PIN BASED PARASITIC ARRAYS (ERPPA)

Thennarasan Sabapathy[1, *], Mohd F. Jamlos[1], R. Badlishah Ahmad[2], Muzammil Jusoh[1], Mohd I. Jais[1], and Muhammad R. Kamarudin[3]

[1]Advanced Communication Engineering Centre (ACE), School of Computer and Communication Engineering, Universiti Malaysia Perlis (UniMAP), Kampus Pauh Putra, Arau, Perlis 02600, Malaysia

[2]School of Computer and Communication Engineering, Universiti Malaysia Perlis (UniMAP), Kampus Pauh Putra, Arau, Perlis 02600, Malaysia

[3]Wireless Communication Centre (WCC), Universiti Teknologi Malaysia, UTM Skudai, Johor 81310, Malaysia

Abstract—In this paper, an electronically reconfigurable beam steering antenna using embedded RF PIN switches based parasitic array (ERPPA) is proposed for modern wireless communication systems that operate at 5.8 GHz frequency. In the proposed antenna, a single driven element is fed by a coaxial probe, while each of the two parasitic elements is integrated with an RF PIN switches that embedded inside the substrate. In the conventional reconfigurable antennas, the RF PIN switches are mounted on narrow slots created on the top or bottom layer of the radiator/parasitic elements, which could lead to the dimensional changes of the antenna and degrade the performance in terms of beam steering and return loss. However, this research proposes an exclusive solution where the RF PIN diodes at parasitic elements are embedded inside the substrate thus no additional slots have to be created to mount the SMCs on the antenna. In this regard, the proposed antenna is highly competent to eliminate the intermodulation effect generated by the RF PIN diodes and the other passive elements associated with the PIN diodes. In this research, extensive investigations revealed that the parasitic element dimension and the selection of RF PIN switches significantly influence

Received 29 April 2013, Accepted 26 May 2013, Scheduled 31 May 2013

* Corresponding author: Thennarasan Sabapathy (thenna84@gmail.com).

the antenna's beam steering capability. Adopting certain ON/OFF condition of the embedded RF switches, three beam-steering angles of $-30°$, $0°$ and $+30^{\circ}$ are achieved in the xz-plane with measured peak gains at $\theta = -30°$, $0°$ and $+30°$ are 6.5 dBi, 6.5 dBi and 4.9 dBi, respectively. The fabricated antenna with Taconic substrate provides a good agreement with the simulation result. Furthermore, the performance of ERPPA is further tested by outdoor measurement using a wireless bridging system to verify the functionality of the designed antenna at the angles of $-45°$, $-30°$, $-15°$, $0°$, $15°$, $30°$ and 45°. The analysis with the switched diversity combining scheme has demonstrated that a maximum diversity gain approximately of 12 dBi is offered by the proposed antenna. With a compact dimension of 32 mm by 76 mm, the proposed antenna is a potential candidate in point-to-point wireless applications such as WIFI application.

1. INTRODUCTION

During the past few decades, with the proliferation of wireless communication technologies tremendous improvement has been witnessed in the radio frequency (RF) and microwave antenna design. The research in the modern wireless communication systems is more focused on identifying appropriate methods and schemes to develop intelligent-like wireless communication systems. In order to combat with various wireless propagation issues such as shadowing, interference, and energy waste, the modern wireless communication system is usually deployed with smart antenna or adaptive reconfigurable antenna at the RF front-end. In physical point of view, these propagation phenomena could be mitigated if the antenna has the capability to steer its main beam towards a desired direction while suppressed the other beam in unwanted directions.

To overcome the issues mentioned above, radiation pattern reconfiguration of an antenna is useful, and conventionally such reconfigurability is obtained through phased array antenna [1, 2]. Such an antenna design involves many subsystems such as an array of antennas, phase shifter and beamforming unit in such a way that the beam can be reinforced to steer in a desired direction [3]. This will result in complex, bulky and increase system cost and weight. However, recent works on reconfigurable antennas have provided an alternative solution to perform the beam steering with less complexity. Such reconfigurable antenna adopts the use of active component like PIN diodes [4–7], varactor diodes [8] and MEMS [9] to control the beam steering/pattern of the antenna. These devices provide switching mechanisms where the current paths and resonant length are altered

to offer beam-reconfigurability.

However, the main drawback of using RF PIN as the switch is that it requires additional passive elements such as the inductor and capacitor for DC biasing circuitry, which severely affects the antenna dimension and efficiency and also in the return loss performance. Additionally, the knowledge on beam-steering effects by the use of different RF PIN and practical solution to improve DC biasing circuitry system is very limited and leave unexplored [4, 5, 10]. However, in this research, the combination of embedded RF PIN diode with DC biasing circuitry at the ground plane has solved those affects and any unnecessary spurious effect that could be generated from the DC biasing wires. In particular, the unique feature offered by the embedded RF PIN technique is that the PIN diodes are inserted inside the substrate thus it tends to avoid much alteration of the parasitic patch dimension while the inductors and capacitors are kept isolated from the parasitic elements in order to minimize the effects towards the beam tilt angle.

On the other hand, existing works using parasitic arrays have only discussed radiation pattern without the analysis on antenna gain [11, 12], and the use of actual RF switch at the fabricated antenna is unimplemented [13]. A design comparable to the embedded RF PIN based parasitic array (ERPPA), which is introduced in this work, is proposed in [14], where a beam steering antenna is designed for 5.6 GHz frequency. The fabricated antenna in that work has shown approximately 8 dBi gain in all steered directions ($\theta = -30°$, $0°$ and $+30°$), but the design has following disadvantages: 1) The antenna has a high complexity level where two layers are required, namely a 5×5 pixel based parasitic layer and a rectangular patch layer. 2) The switching network has to be separated from the array elements and a large amount of 20 switches are required to perform the reconfigurability. 3) The prototype of the antenna design with actual switches is not presented. 4) The overall size is 60 mm by 60 mm.

However, the proposed ERPPA antenna in this work has successfully achieved comparable measured gain of 6.5 dBi with the advantages as follows; 1) The physical structure of the ERPPA is compact and has a smaller dimension of 32 mm by 76 mm (33% of reduction). 2) The design complexity is reduced where the novel embedded RF PIN technique is proposed to simplify the DC biasing circuitry. This new approach in implementing the surface mount components (SMC), such as PIN diode and lump elements by properly arranged with a unique geometry resulted in better antenna performance by ensuring a smooth RF current flow and DC current flow in desired directions and block them in unwanted directions. and

3) In contrast to [14] which used 20 switches to achieve beam-steering at ($\theta = -30°$, 0° and +30°) directions, the proposed ERPPA only uses 2 switches to perform the beam steering at those similar directions.

This paper presents an electronically reconfigurable beam-steering antenna with a novel DC biasing circuitry geometry that achieves good steering angle and, in contrast to existing RF PIN based designs, requires a low complexity. The novelty of the design lies in the exclusion of the majority of the DC-biasing components from the front panel of the antenna that successfully eliminate the intermodulation effect generated due to the RF PIN diodes and the other passive elements associated with the PIN diodes. The preliminary concept of beam-steering with parasitic patch is described in depth in Section 2. The challenge of integrating DC biasing circuit over the concept proven antenna is explained in Section 3. Following the best PIN diode identified by the thorough investigation in Section 3, Section 4 continues with the fabrication of the ERPPA operating at 5.8 GHz frequency and it tested experimentally. Section 5 provides the analysis of practical usability of the antenna with an outdoor environment test. Finally, some concluding remarks are given in Section 6.

2. STAGE 1: PROOF OF CONCEPT

In this section, a preliminary investigation of beam steering with parasitic patch is carried out in depth. The effect of the parasitic patch size and element spacing is presented. Thus to proof the switching concept, the RF PIN switch at the antenna's structure has been replaced with metal pins with a diameter of 1 mm and height of 1.6 mm. The present and absent of the metal pin is considered ON and OFF state, respectively.

2.1. The Physical Structure and the Radiation Mechanism of the Antenna

Figure 1 illustrates the physical structure of the beam-reconfigurable parasitic array antenna. The antenna consists of three parallel patches on a full grounded Taconic dielectric substrate with a thickness of 1.6 mm and a dielectric constant (ε_r) of 2.2. The center rectangular patch has a width of W mm and length of L mm. This is the driven element of microstrip array where it is fed through a subminiature (SMA) probe from the back of the antenna. The feed location a is optimized to achieve a desired input impedance. The parasitic elements are smaller with respect to the driven element where the width and length are denoted as W' and L', respectively. Each parasitic

element has a switch connected to the ground plane at the back of the antenna. This switch can be considered as a shorting pin. The location of the switch is crucial in determining the optimum tilt angle. As depicted in Figure 1, the switch is located at the height of u mm from the bottom of the parasitic patch and v mm from the outer side of the parasitic patch. Both parasitic elements are physically the same electrical length, switching their states between short-and open circuited results in a variation of the elements' electrical length. Thus, when the switch/shorting pin is short to the ground (ON state, via is active), it acts as a reflector (R). In contrast, when the switch is open (OFF state, via is inactive) it acts as a director (D). This principle of antenna operation is much like a Yagi-Uda antenna set on a dielectric substrate backed by a finite ground plane. The size of the substrate dimension and the ground plane is optimized in order to achieve optimum beam tilt angle and similar gain in all beam-steered directions. A comprehensive treatment on the Yagi-Uda concept can be found in [15].

Overall, this antenna works in three modes, namely RD (left parasitic is R and right parasitic is D), DR (left parasitic is D and right parasitic is R), and DD (both parasitics are D) modes. In

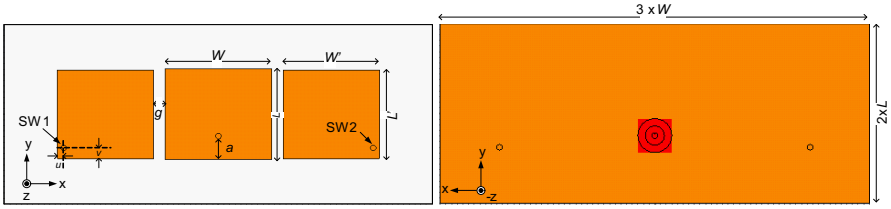

Figure 1. The physical structure of the antenna used in simulation during the preliminary investigation. (a) Front view. (b) Back view.

Table 1. Beam steering characteristic of the proposed antenna based on the switching condition.

Switch Operation		**Mode of Operation**
SW1	SW2	
ON	OFF	RD
OFF	ON	DR
OFF	OFF	DD

these configurations, the coupling between the driven element and the two parasitic elements controls the radiation patterns. The switching conditions of SW1 and SW2 paired with the respective mode are tabulated in Table 1. In what follows, a detailed description of the antenna design with the related analyses and results will be presented.

2.2. Design and Analysis of the Proposed Antenna

To demonstrate the beam-reconfigurability of this method, an antenna is designed for 5.8 GHz frequency. After extensive parametric studies through simulations, the optimum physical parameters obtained for this antenna are as follows: $W = 16\,\text{mm}$, $L = 11.3\,\text{mm}$, $W' = 0.9 \times W\,\text{mm}$, $L' = 0.98 \times L\,\text{mm}$, $a = 2.85\,\text{mm}$, $u = 3.4\,\text{mm}$ and $v = 1.48\,\text{mm}$. These parameters are obtained using CST Microwave Studio with the maximum tilt angles are achieved in DR and RD mode.

2.2.1. Reflection Coefficient and Radiation Pattern of the Three Different Modes

Figure 2(a) shows the reflection coefficient (S_{11}) obtained for all three modes. As one can expect, due to symmetric size and location of the switches, both RD-mode and DR-mode yields similar result in terms of S_{11} and both achieved S_{11} less than $-10\,\text{dB}$. A detailed observation could clarify that in the DD-mode the antenna could only achieve a reflection coefficient of $-8\,\text{dB}$. However, for an antenna with a good beam steering characteristics which can provide a large beam tilt angle,

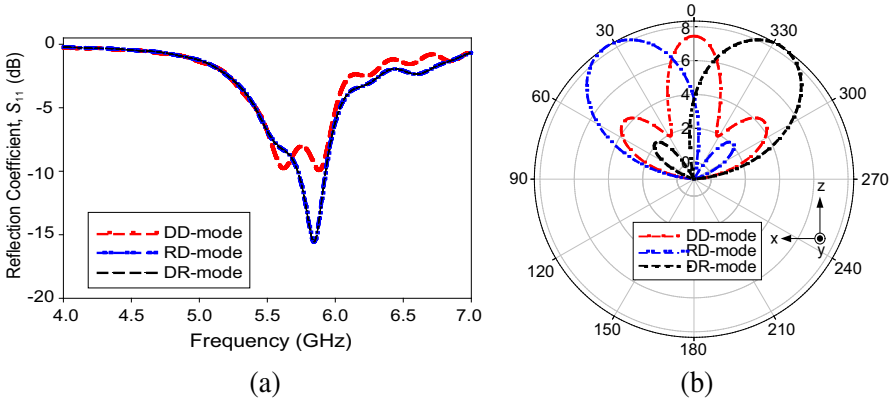

Figure 2. Simulation results of (a) reflection Coefficient and (b) radiation pattern for three different modes of operations.

a tolerable return loss is sufficient. A minimum return loss of 6 dB is considered adequate to have tolerable impedance matching and power transfer for an antenna with beam steering characteristics [16]. In that case, regardless of the switching modes at 5.8 GHz operation, the proposed antenna maintains reflection coefficient of less than −10 dB for RD and DR-modes and less than −8 dB for the DD-mode.

Along with the reflection coefficient, the radiation patterns of the antenna at three different modes are depicted in Figure 2(b). Based on the switches configuration, three different directive radiation patterns are obtained at −33°, 0° and +33° along the x-axis. The maximum gain for the radian pattern steered to $-x$-axis and $+x$-axis is 8.2 dBi, while the peak gain for the main beam steered at 0° is 7 dBi. The result also confirmed that at least 6 dBi of gain can be obtained from −53° to +53°. The results from this Section justify the functionality of this antenna at 5.8 GHz with a good beam steering capability.

2.2.2. Influence of the Spacing between Parasitic Element and Driven Element

The spacing between the parasitic element and driven element g is identified as an important factor in obtaining good beam scanning. The radiation pattern results shown in Figure 3(a) demonstrate the effect of g. It proves that regardless of g, the tilt angle (−30°) is not much affected. However, we can clearly observe that the side lobe level increases as the g increases. In order to direct the beam to a desired direction and avoid unwanted interferences, it is important to consider the side lobe level of the radiation pattern. In that case, g is chosen as 2 mm to give tolerable radiation pattern. In simulation, it has been identified that when the size of g smaller than 2 mm, the reflection coefficient is altered, thus it is kept as low as 2 mm.

On the other hand, a detailed analysis has been carried out to show the effect of the parasitic element size towards the beam tilt angle. From the analysis, it has been identified that the parasitic element size should be slightly smaller than the center driven element. Figure 3(b) shows that the decrement of length L' contributed to the degradation of the optimum beam tilt angle. When length $L' = 0.98 \times L$ mm maximum beam steering achieved −32°, when $L' = 0.97 \times L$ mm the main beam direction is at −30°, when $L' = 0.96 \times L$ mm the main beam direction is at −28° and when $L' = 0.95 \times L$ mm the main beam direction is at −25°. In the final design, the parasitic element length is chosen as $0.98 \times L$ mm since it gives the best compromise between the tilt angle and the side lobe level.

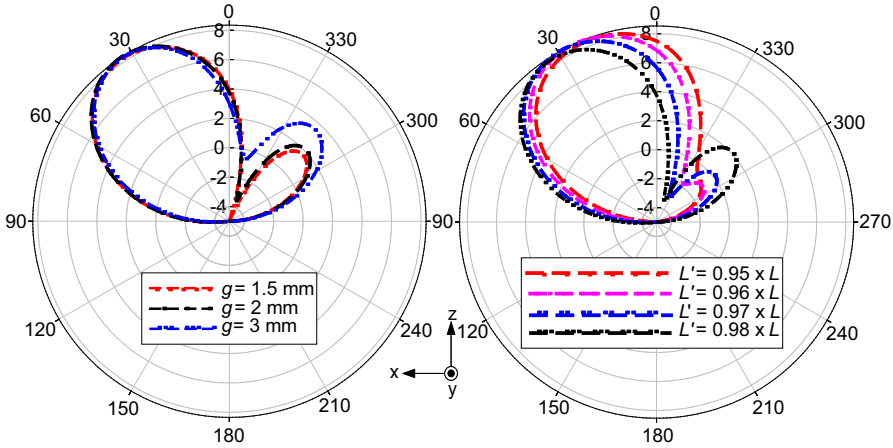

Figure 3. Radiation pattern of beam scans for a different dimension of (a) element gap, g and (b) parasitic height, L'.

3. STAGE 2: DESIGN AND ANALYSIS WITH DC BIASING

In this section, the finalized design is presented where the DC biasing circuitry is introduced. In particular, the geometry of the DC biasing circuit is considered novel in this work where the RF PIN is embedded inside the substrate to avoid much alteration at the parasitic patch, in order to minimize the effects towards the beam tilt angle.

3.1. Modified Physical Structure of the Antenna to Integrate DC Biasing Circuitry

The main disadvantage of employing PIN diode as the RF switch is that it needs additional lumped elements such as the inductor and capacitor for DC biasing circuitry which could disrupt the antenna dimension and performance.

However, the proposed design geometry of the DC biasing circuitry solves this design issue. Figure 4 illustrates the antenna design along with little modification for the DC biasing purpose. At the ideal location of shorting pin, an RF PIN is embedded, then an RF choke/inductor is connected to the $+ve$ terminal of the diode. It can be seen from Figure 4(a), the inductors $L1$ and $L2$ are connected to V_{DC} and their function is to isolate the RF current from the antenna to flow to the DC biasing line. Unlike in previous works [5], which

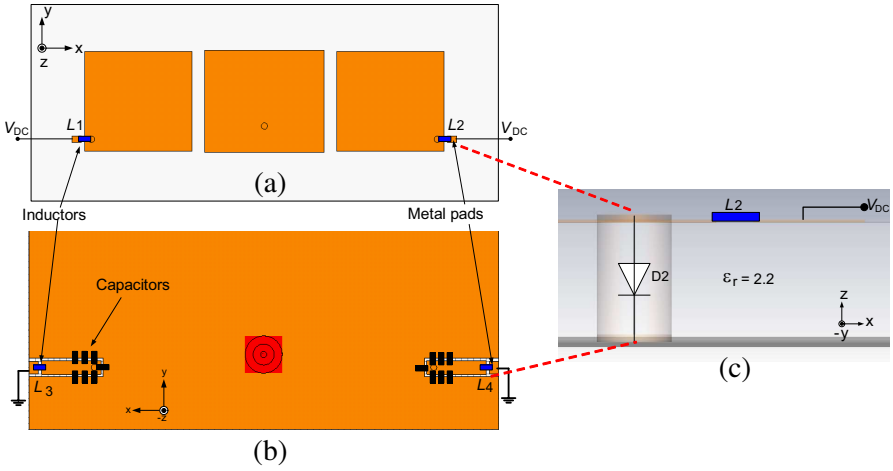

Figure 4. The physical structure of the ERPPA using a novel DC biasing circuit geometry. (a) Front view. (b) Back view. (c) Side view — Parasitic element embedded with RF PIN diode.

involved with RF PIN switch, the DC biasing wires in this work are isolated from the radiator of the antenna. This makes the design simple and avoids any unnecessary spurious effect that could be generated from the DC biasing wires. The *-ve* terminal of the embedded diode is directly connected to the ground plane of the antenna with the help of embedded RF pin technique proposed in this work. A clear insight of the proposed antenna with embedded RF PIN can be found through Figure 4(c). A 1 mm diameter hole is drilled through the substrate at the shorting location, and then the PIN is inserted. A careful observation at the front panel of the antenna can reveal that the parasitic element is isolated from the driven element. Therefore, the use of DC blocking capacitor is not necessary at that location.

However, at the ground plane, the antenna's reflector is shared by the driven element and the parasitic elements. In such a scenario, the DC current is unblocked and can flow in the antenna through the ground plane. Therefore, the DC biasing circuitry at the ground plane is considered crucial. To resolve this design issue, the shorting locations of the each switch are isolated from the main reflector with a narrow slot with a width of 0.4 mm as depicted in Figure 4(b). With the proposed dimension, each switch's DC operation will not be affected and the DC bias line can be isolated from the RF path of the antenna. After that, a DC blocking capacitor should be added to allow the RF current flow and block the DC current. However in this design, a

number of 100 pF DC capacitors are added in order to ensure a smooth RF current flow from the main reflector to the parasitic element. On the other hand, inductors $L3$ and $L4$ are connected between the *-ve* terminal of the diode and the DC_ground to ensure the RF current path from the antenna to DC biasing line is blocked. Note that all inductors' value is 27 nH.

3.2. The Choice of RF PIN Diode against the Operating Frequency of the Antenna

Important consideration needs to be taken into account when choosing the suitable PIN diode especially when the antenna deals with beam steering. This is due to the fact that the actual PIN diode switch is very different from the ideal switch that assumed in the previous section. At ON condition, the diode can be represented as a RL series circuit and at OFF condition the switch can be considered as an RC shunt circuit. For good OFF condition, the shunt capacitor should be very low thus it will provide good isolation loss where RF leakage through the diode at OFF state will be minimized. This RL and RC representation can be represented in CST along with the designed antenna to give an accurate result. Apart from this method, a better simulation analysis which produces results that is more accurate can also be made with the help of touchstone block which contains s2p file. The s2p file consists of *s*-parameter information of the diode for the ON and OFF condition. This file can be obtained from the manufacturer and can be included in simulation to give results that is more accurate. First, this work adopted the use of BAR50-02L diode for the proposed antenna. The result from simulation shows that at 5.8 GHz frequency, this diode unable to achieve the desired beam-steering characteristic.

In particular, Figure 5(a) shows that using this diode for antenna operating at 5.8 GHz frequency, the desired radiation pattern for DD-mode is unattainable. Furthermore, the side-lobe level at RD and DR modes are very high compared to the results from the ideal switch mechanism that studied in Section 2. To further verify the functionality of the diode at lower frequency, another design that operates at 5 GHz is constructed and the similar simulation procedure with touchstone block performed. As shown in Figure 5(b), at this frequency the antenna able to perform beam steering but with a little performance drop and some minor optimization required with L' to enable the beam steering. Apart from that, it also can be noticed that the beam tilt angle has dropped about 4 degrees in both RD and DR modes.

However, the original objective of this paper is to obtain the beam steering at 5.8 GHz frequency. Therefore, another RF PIN

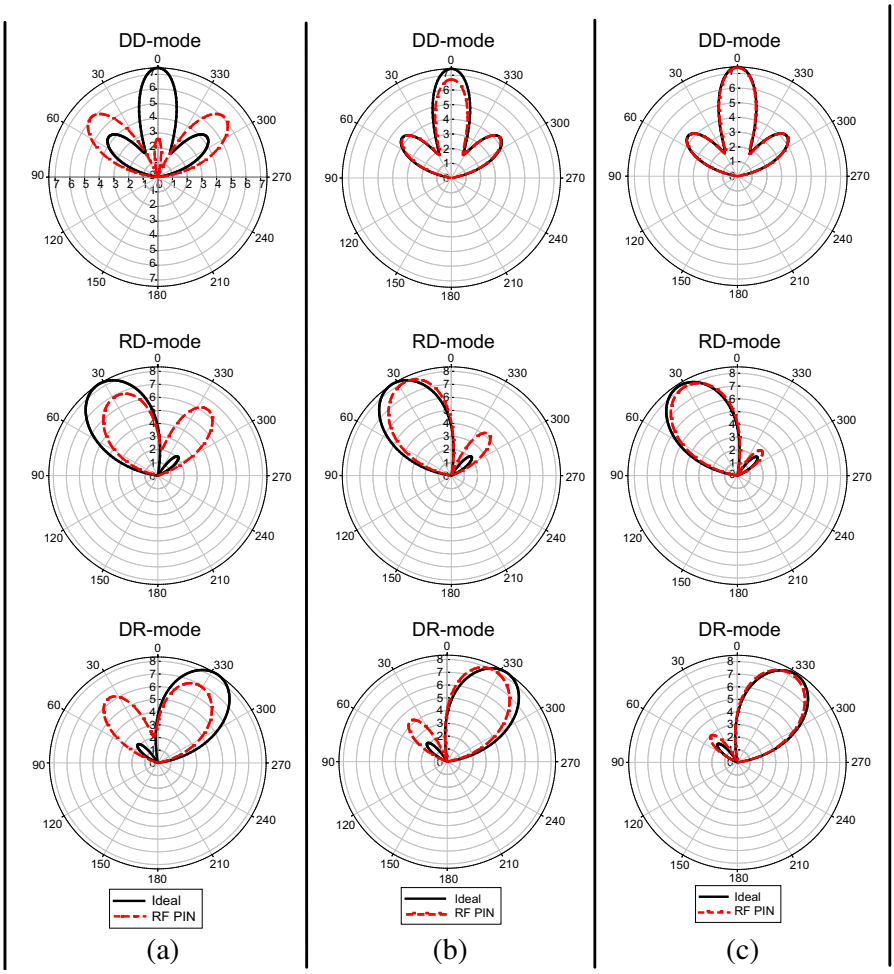

Figure 5. Comparisons of beam steering result using ideal switch and RF PIN. (a) 5.8 GHz antenna with BAR. (b) 5 GHz antenna with BAR50-02L. (c) 5.8 GHz with HPND-4005.

diode known as HPND-4005 is chosen for analysis. This diode is well known for its extremely low capacitance for its OFF state and can support frequency up to 18 GHz, small in size and provides high isolation loss at OFF state [17]. According to the technical data sheet provided by the manufacturer, the HPND-4005 PIN diodes are simulated as 4.6-Ω resistor and 0.017-pF capacitor in the ON and OFF states respectively [18]. The investigation reveals that the HPND-4005

provides superior performance compared with BAR for the antenna operating at 5.8 GHz. Figure 5(c) shows that beam steering result for the antenna using HPND-4005 almost identical to the ideal switching condition.

In fact, a clear insight of the phenomena occurred due to the different PIN diodes used in simulation can be explained by the isolation loss (ISO) of the RF PIN switch at OFF state. Figure 6 shows the series connected switch element (in the red dotted box) in a single pole-single throw (SPST) switch topology. At OFF state, the isolation loss of a series switch can be given as follows [19],

$$\mathrm{ISO} = 10\log\left[1 + \left(\frac{1}{2\pi f \cdot C_s \cdot Z_0}\right)^2\right] \tag{1}$$

where f denotes the frequency, C_s represents the off-state capacitance and Z_0 is the source/load impedance, respectively. At 5.8 GHz frequency, the ISO of the BAR50-02L is obtained through the technical datasheet provided by the manufacturer [20]. The ISO of this diode at $Z_0 = 50\,\Omega$ is approximately 11 dB.

As for the HPND-4005, the datasheet only provides the typical C_s for OFF state which is 0.017 pF. In that case, the ISO for HPND-4005 can be calculated using Equation (1) and it gives 24 dB. When the ISO is low, the open circuit provided by the BAR50-02L RF PIN is not very effective, thus some RF leakage is still possible. For instance, in RD-mode, the RF leakage at SW2 will lead to ineffectiveness of the director (D) in the parasitic element, thus it behaves much like the reflector (R), and so it will push the beam in the opposite direction. In such a scenario, the side-lobe level increases in the obtained beam steering (RD-mode) as shown in Figure 6(a). Overall, HPND-4005 provides better ISO at 5.8 GHz frequency, thus it is more suitable for the proposed ERPPA. As for the BAR PIN diode, it is suitable for frequency operating at 5 GHz. The better result is expected for antenna made at a lower operating frequency since the isolation loss is higher at lower frequencies, for instance, the technical data sheet provides that the ISO is 20 dB at 1.8 GHz frequency.

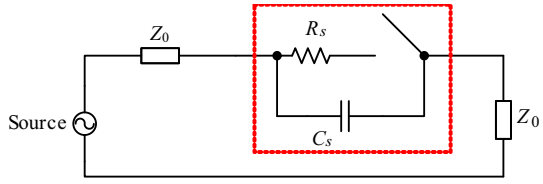

Figure 6. Representation of a switch with lumped elements.

4. EXPERIMENTAL ANALYSIS WITH THE FABRICATED ANTENNA

Following the thorough investigation and analysis conducted in Section 3, HPND-4005 is used for the fabrication of the proposed antenna operating at 5.8 GHz frequency. Figure 7 shows the photograph of the fabricated antenna. The diode is embedded inside the substrate, thus it cannot be viewed. The inductor can be observed in the front view of the antenna and the inductor with capacitors can be seen in the rear view of the antenna.

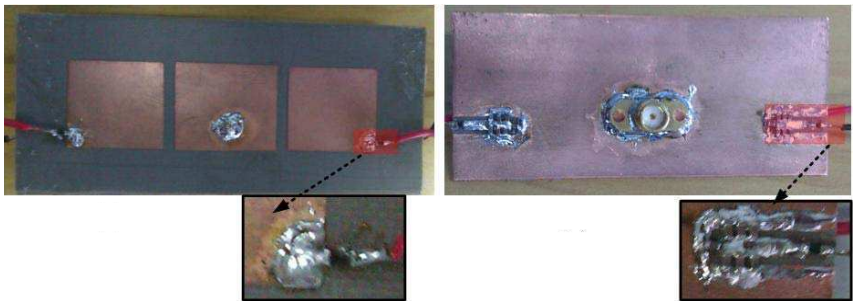

Figure 7. Photograph of the fabricated antenna. (a) Front view. (b) Rear view.

4.1. Measurement of the Reflection Coefficient (S_{11})

Figure 8(a) demonstrates that the fabricated antenna has successfully achieved a minimum reflection coefficient of less than −10 dB ($S_{11} < -10$ dB) for all three modes from 5.771 GHz to 5.934 GHz. The measured reflection coefficient has slightly shifted to the higher frequency of 10 MHz with greater return loss compared to the simulated responses as in Figure 8(b). This variation could be due to the fabrication tolerance, material loss, SMA connector and the actual DC biasing circuitry.

4.2. Radiation Pattern Result

The radiation pattern measurement was performed in an anechoic chamber, property of the Antenna and Microwave Lab (Amrellab) of Universiti Malaysia Perlis with the help of Agilent Technologies E5071C (9 kHz to 8.5 GHz) Network Analyzer. Figure 9 shows the

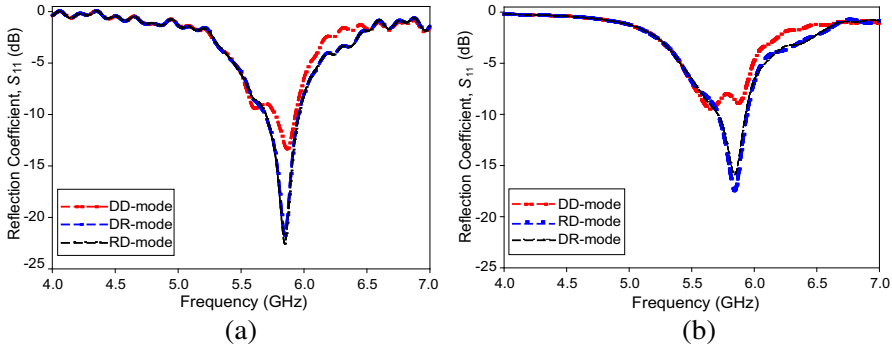

Figure 8. Reflection coefficient of the proposed antenna. (a) Measurement. (b) Simulation.

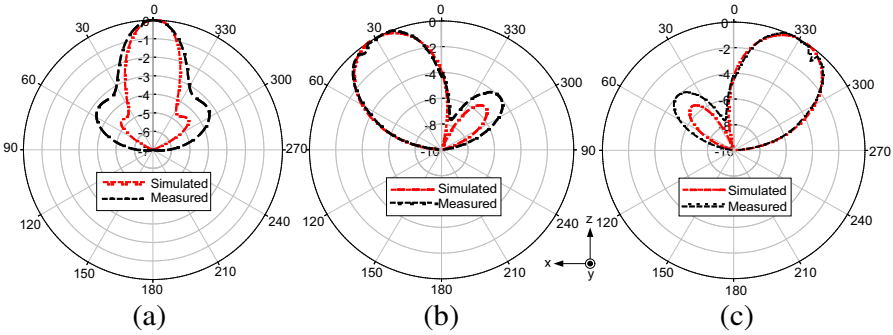

Figure 9. Radiation pattern comparison of the proposed antenna (a) DD-mode. (b) RD-mode. (c) DR-mode.

comparison results of the simulated and measured radiation pattern for each PIN diode switch configuration. The polar graph results are normalized to their peak values to ease the comparison of the tilt angle and side lobe level of the simulation and measurement results.

It can be seen that all three modes achieves almost similar measurement result compared to the simulation result. The only difference that can be observed is that the side-lobe level of measurement is higher compared to the simulation result.

The overall radiation pattern results which consist of beam tilt angle and peak gain in each direction are presented in Table 2. In particular, the table presents the simulation results of the antenna with ideal switch, the simulation results of the antenna with simulated HPND-4005 switch and measurement results with actual HPND

Table 2. PIN diode switches configuration of the proposed beam steering antenna.

Modes	**Tilt angle** (θ_m)		
	Simulation (Ideal switch)	Simulation (Actual switch)	Measurement
RD	$-33°$	$-30°$	$-30°$
DR	$+33°$	$+30°$	$+30°$
DD	$0°$	$0°$	$0°$
Modes	**Maximum Gain** (dBi)		
	Simulation (Ideal switch)	Simulation (Actual switch)	Measurement
RD	8.2	7.3	6.5
DR	8.2	7.3	6.5
DD	7.0	5.6	4.9

switch. It shows that, the beam tilt angle and the gain for RD and DD mode has dropped about 3° after the HPND switch is adopted in the simulated antenna. Similar trend can be observed at the peak gain where it has also dropped for all three modes. This proves that, in simulation it is necessary to include all the information of actual switch and associated SMCs that will be used in practical design to have a more accurate result. The fabricated design offers similar beam tilt angle but with an average gain drop of 1 dB compared with the simulation result. The slight discrepancies of simulation and measurement result could be resulted due the RF signal absorption caused by the actual SMCs in the fabricated design. Overall, the measured results show that the antenna can steer the beam up to three directions, $-30°$, $0°$ and $+30°$ with respective peak gain of 6.5 dBi, 4.9 dBi and 6.5 dBi.

5. PRACTICAL ANTENNA MEASUREMENT USING HIGH SPEED WIRELESS BRIDGING SYSTEM

In this section, the practical use of the ERPPA is presented through an analysis in outdoor measurement. The received power measurement is conducted using a high speed wireless bridging system that uses the 5.8 GHz band as the bridge and 2.4 GHz band as the access point. The wireless bridge has employed two stations, Station A and Station B.

As shown in Figure 10(b), the Station A is connected to a router that provides internet connections. Apart from that, it can be noticed that a laptop is also connected to the router and it acts like a network monitoring system. The network monitoring system is assisted with an interface called WinBox where various network parameters such as transmitted power, received power, bandwidth and data rate could be observed. In this work, we are interested in monitoring the power received by the antenna at Station B to verify the performance of the proposed antenna at outdoor environment.

The fabricated antenna is deployed at Station A, and a highly directional antenna is fixed at Station B. The Station B is located at various points as depicted in Figure 10(a) up to 15 m and at angles from $-45°$ to $45°$ with a step size of $15°$. Station B requires portability during measurement; therefore it is powered up with a smart power bank. Since the three directive beam patterns are ranging from $-30°$ to $+30°$, the measurement is limited from $-45°$ to $45°$. Using WinBox, the transmit power of the Station A is set to +17 dBm and the bridge is set to 5805 MHz channel. The height of the antenna at Station A and Station B is kept aligned in order to minimize the multipath effect, thus allows the signal degradation is only caused by the path loss [4]. The received power measurement is carried out for all three modes of the

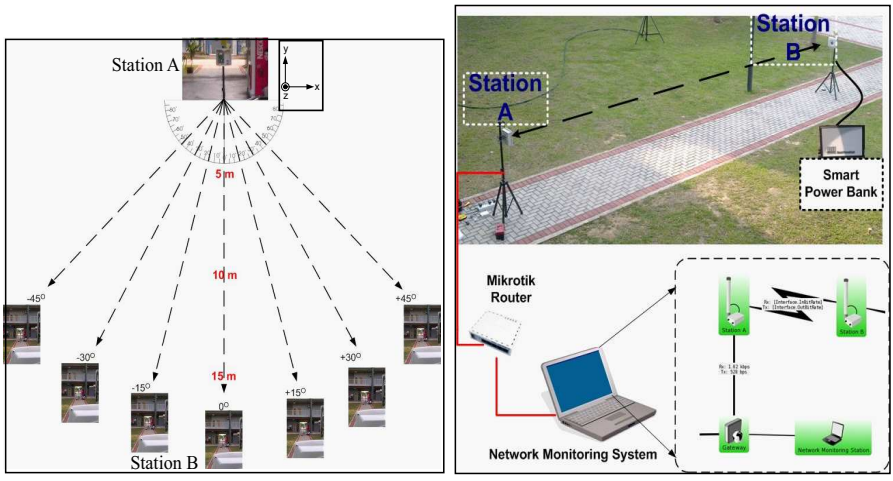

Figure 10. Measurement setup. (a) Measurement for different angles and distances. (b) Illustration of outdoor measurement setup with network monitoring system.

proposed antenna, RD, DR and DD modes. The outdoor measurement is limited at line-of-sight (LOS) environment to verify the functionality of the beam steering of the antenna and it is ensured that no significant effect from any electromagnetically objects thus the effect of unwanted propagation characteristics influence the measurement.

5.1. Verification of Beam-steering with Received Power Measurement

Figure 11(a) shows the received power by Station B when the ERPPA at Station A operates at RD-mode. As expected, the measurement at $-30°$ has recorded maximum received power. For instance, the distance of 5 m generates the received power of approximately -17.5 dBm. It can be noticed that the received power decreases when the Station B is moved away from the $-30°$, either to positive or negative direction. However, it can be observed from Figure 11(b) that the received power increases drastically at $-45°$. This is due to the effect of the low side-lobe level of the proposed antenna as can be seen in Figure 9(c). This has proven the practical use of the antenna at outdoor environment where the beam steering capability of the proposed antenna performs similar to the one measured using an anechoic chamber as described in Section 4.2. Similar performance has been observed for other two modes where the received power showed the highest value at the beam-steered angles of $0°$ and $+30°$ for DD and DR modes respectively.

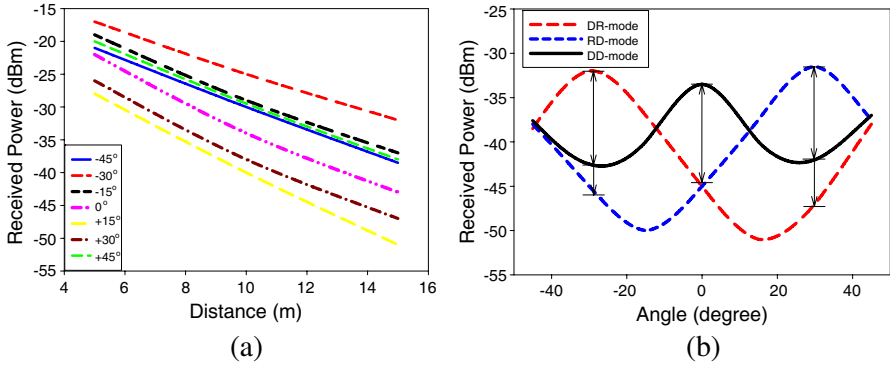

Figure 11. (a) The received power at Station B when the ERPPA at Station A activated with the RD-mode. (b) The received power at Station B for different modes of operation at 15 m.

5.2. Outdoor Diversity Performance of the Proposed Antenna

This section investigates the diversity property of the proposed antenna with the analysis of received power measurement. Figure 11(b) shows the received power at the distance of 15 m against the different angle of arrivals. The arrows show the maximum diversity gain available when the antenna changes from one mode to another mode. This gain can be obtained by assuming the antenna adopts switched diversity combining method [21]. The switched diversity combining scheme allows only one signal to be used at a particular direction. When such a signal sufficiently falls below the threshold level, it then switches to another direction which produces the strongest signal. The feasibility of this method shows that it is suitable for the pattern diversity antenna where only one beam can be used at a time. Such methods are also used in cell-site diversity application [22] where the main beam steered towards a desired direction while suppressing the signals from the unwanted directions. Therefore, the study on the diversity gain based on pattern diversity is considered important to highlight the capability of the antenna in the outdoor environment. The maximum diversity gains achievable when the antenna switches from one mode to another mode are tabulated in Table 3. The results show that the proposed ERPPA is capable of having an average maximum diversity gain of 12 dBi for all states. Generally, the diversity gain will be lower if the beamwidth of each directive pattern is large [23]. However, the narrow beam pattern of the each ERPPA mode provided this diversity gain enhancement.

Table 3. Antenna diversity gain for beam-steering characterized by the different state of operations.

Steering direction	Present State	Next State	Diversity Gain
Towards −30°	DR	RD	12.8
	DD	RD	10.5
Towards 0°	RD	DD	11.5
	DR	DD	11.4
Towards +30°	DD	DR	14.5
	RD	DR	10.5

6. CONCLUSION

This paper presents an electronically reconfigurable beam steering antenna using a novel embedded RF PIN based parasitic array (ERPPA) for 5.8 GHz operating frequency. The salient feature of the proposed antenna is that the complexity of the design with DC biasing circuitry is reduced through embedded RF pin technique to maintain the compact size while meeting the beam-steering angle requirements obtained from the *proof of concept* design. Using only two sets of embedded RF PIN switches, the current flow can be controlled to perform the parasitic elements as a director or reflector which leads to the reconfigurable beam steering capability, where such a behavior is similar to the Yagi-Uda concept. The size of parasitic elements and the spacing between the elements play important role in determining the better tilt angle and lower side-lobe level. Furthermore, a clear insight of RF switch is presented with different choice of RF PIN and the relationship of the PIN between isolation loss, the frequency and beam-steering characteristics are described in depth. Through certain RF PIN configuration, the proposed antenna is able to steer its directive beam pattern to three different directions at $\theta = -30°$, $0°$ and $+30°$ with an average peak gain of ~ 6 dBi in all directions. Initial investigation through simulation has identified that the beam scanned angles at different directions such as $10°$ and $20°$ can be achieved but with increased complexity of the design. The fabricated antenna is capable to operate in the frequency range of 5.771 GHz to 5.934 GHz under tolerable $S_{11} < -10$ dB. Analysis through outdoor measurement shows that the proposed ERPPA maintains an average maximum diversity gain of ~ 12 dB for all states of operation. With a compact dimension of 32 mm $\times$ 76 mm, the ERPPA is suitable for various portable and fixed wireless applications such as WiFi.

REFERENCES

1. Sanyal, S. K., Q. M. Alfred, and T. Chakravarty, "A novel beam-switching algorithm for programmable phased array antenna," *Progress In Electromagnetics Research*, Vol. 60, 187–196, 2006.
2. Expósito-Domínguez, G., J.-M. Fernández González, P. Padilla de la Torre, and M. Sierra-Castañer, "Dual circular polarized steering antenna for satellite communications in x band," *Progress In Electromagnetics Research*, Vol. 122, 61–76, 2012.
3. Yuan, T., N. Yuan, J. L.-W. Li, and M.-S. Leong, "Design and analysis of phased antenna array with low sidelobe by fast

algorithm," *Progress In Electromagnetics Research*, Vol. 87, 131–147, 2008.

4. Jusoh, M., M. F. B. Jamlos, M. R. Kamarudin, T. Sabapathy, M. I. Jais, and M. A. Jamlos, "A fabrication of intelligent spiral reconfigurable beam forming antenna for 2.35–2.39 GHz applications and path loss measurements," *Progress In Electromagnetics Research*, Vol. 138, 115–131, 2013.
5. Jais, M. I., M. F. B. Jamlos, M. Jusoh, T. Sabapathy, M. R. Kamarudin, R. B. Ahmad, A. A. A.-H. Azremi, E. I. Bin Azmi, P. J. Soh, G. A. E. Vandenbosch, and N. L. K. Ishak, "A novel 2.45 GHz switchable beam textile antenna (SBTA) for outdoor wireless body area network (WBAN) applications," *Progress In Electromagnetics Research*, Vol. 138, 613–627, 2013.
6. Kang, W., K. H. Ko, and K. Kim, "A compact beam reconfigurable antenna for symmetric beam switching," *Progress In Electromagnetics Research*, Vol. 129, 1–16, 2012.
7. Peng, H.-L., W.-Y. Yin, J.-F. Mao, D. Huo, X. Hang, and L. Zhou, "A compact dual-polarized broadband antenna with hybrid beam-forming capabilities," *Progress In Electromagnetics Research*, Vol. 118, 253–271, 2011.
8. Ojefors, E., C. Shi, K. From, I. Skarin, P. Hallbjorner, and A. Rydberg, "Electrically steerable single-layer microstrip traveling wave antenna with varactor diode based phase shifters," *IEEE Transactions on Antennas and Propagation*, Vol. 55, 2451–2460, 2007.
9. Petit, L., L. Dussopt, and J. M. Laheurte, "MEMS-switched parasitic-antenna array for radiation pattern diversity," *IEEE Transactions on Antennas and Propagation*, Vol. 54, 2624–2631, 2006.
10. Jamlos, M. F., T. A. Rahman, M. R. Kamarudin, P. Saad, O. A. Aziz, and M. A. Shamsudin, "Adaptive beam steering of rlsa antenna with RFID technology," *Progress In Electromagnetics Research*, Vol. 108, 65–80, 2010.
11. Zhang, S., G. H. Huff, J. Feng, and J. T. Bernhard, "A pattern reconfigurable microstrip parasitic array," *IEEE Transactions on Antennas and Propagation*, Vol. 52, 2773–2776, 2004.
12. Preston, S. L., D. V. Thiel, J. W. Lu, S. G. O'Keefe, and T. S. Bird, "Electronic beam steering using switched parasitic patch elements," *Electronics Letters*, Vol. 33, 7–8, 1997.
13. Ha, S.-J. and C.-W. Jung, "Reconfigurable beam steering using a microstrip patch antenna with a u-slot for wearable fabric

applications," *IEEE Antennas and Wireless Propagation Letters*, Vol. 10, 1228–1231, 2011.

14. Li, Z., H. Mopidevi, O. Kaynar, and B. A. Cetiner, "Beam-steering antenna based on parasitic layer," *Electronics Letters*, Vol. 48, 59–60, 2012.
15. Zhao, S.-C., B.-Z. Wang, and W. Shao, "Reconfigurable Yagi-Uda substrate for RCS reduction of patch antenna," *Progress In Electromagnetics Research B*, Vol. 11, 173–187, 2009.
16. Nair, S. and M. J. Ammann, "Reconfigurable antenna with elevation and azimuth beam switching," *IEEE Antennas and Wireless Propagation Letters*, Vol. 9, 367–370, 2010.
17. Boudaghi, H., M. Azarmanesh, and M. Mehranpour, "A frequency-reconfigurable monopole antenna using switchable slotted ground structure," *IEEE Antennas and Wireless Propagation Letters*, Vol. 11, 655–658, 2012.
18. Jose, S., "HPND-4005 beam lead PIN diode, Datasheet," Avago Technologies, CA, 2006.
19. Rizzi, P. A., *Microwave Engineering: Passive Circuits*, Prentice Hall, 1988.
20. "Silicon PIN diodes, BAR-50," Infineon Technologies AG, Munich, Germany, 2009.
21. Kamarudin, M. R., Y. I. Nechayev, and P. S. Hall, "Onbody diversity and angle-of-arrival measurement using a pattern switching antenna," *IEEE Transactions on Antennas and Propagation,* Vol. 57, 964–971, 2009.
22. Sabapathy, T., S. W. Tan, and T. C. Chuah, "Fuzzy weight controller based cell-site diversity for rain fading mitigation in LMDS networks in the tropics," *Progress In Electromagnetics Research B*, Vol. 28, 235–251, 2011.
23. Lempiainen, J. J. A. and K. I. Nikoskinen, "Signal correlations and diversity gain of two-beam microcell antenna," *IEEE Transactions on Vehicular Technology*, Vol. 47, 755–765, 1998.